Journal of Applied Polymer Science

A comparative study on different rubbery modifiers: Effect on morphologies, mechanical, and thermal properties of PLA blends

Jinian Yang,[1] Shibin Nie,[2] Jinbo Zhu[1]

[1]School of Materials Science and Engineering, Anhui University of Science and Technology, Huainan, 232001, People's Republic of China
[2]School of Mining and Safety Engineering, Anhui University of Science and Technology, Huainan, 232001, People's Republic of China
Correspondence to: S.-B. Nie (E-mail: nsb@mail.ustc.edu.cn)

ABSTRACT: To improve the impact toughness of poly(lactic acid) (PLA), four kinds of rubbery modifiers, including ground tyre rubber (GTR), styrene-butadiene-styrene block copolymer (SBS), ethylene-α-octene copolymer (EOC) and glycidyl methacrylate grafted EOC (mEOC), were introduced for fabricating the PLA blends. The morphological structures, mechanical properties, thermal stability and thermal decomposition kinetics of pristine PLA and the blends were investigated. Results showed that representative droplet-matrix structures were observed in the PLA blends, of which the PLA/SBS blend presented the smallest domains while PLA/EOC case had the largest elastomeric particle size. Accordingly, the highest impact toughness and elongation at break were achieved by PLA/SBS blend, whereas the tensile strength and elastic modulus for the blends were all lower than that of pristine PLA. Though the incorporation of rubbery modifiers barely altered the peak temperature of melting, the degrees of crystallinity for blends were declined sharply. The results of thermo gravimetric analysis indicated thermal degradation process of PLA phase was accelerated by rubbery modifiers and evidenced by the relative higher mass conversion at peak temperature. The reaction order of PLA phase for blends calculated by Carrasco method exhibited similar values when compared with control sample. However, the values of activation energy were rather lower than that of pure PLA. © 2016 Wiley Periodicals, Inc. J. Appl. Polym. Sci. **2016**, *133*, 43340.

KEYWORDS: blends; degradation; elastomers; kinetics; thermoplastics

Received 26 September 2015; accepted 11 December 2015
DOI: 10.1002/app.43340

INTRODUCTION

Poly(lactic acid) (PLA) was a bio-based polymer which could be derived from the renewable sources (corn and starch). It was characterized by excellent biodegradability and biocompatibility, good transparency, as well as superior comprehensive performances than other conventional biodegradable polymers. Now, PLA has been one of the most promising materials for the alternative of petroleum based polymers in plastic industry.[1,2] However, just like other semi-crystal polymers, the inherent brittleness and poor impact toughness would significantly impede its applications, despite that PLA showed the comparable tensile strength and modulus to that of general polypropylene (PP) and polyethylene (PE),[3,4] Therefore, it was rather essential to improve the ductility of PLA products for their broader applications, especially utilized in situations that toughness and impact resistance were crucial.[5,6]

Several useful strategies[6–20] have been proposed and developed to improve the ductility and toughness of PLA, and among which, the melt-blending with flexible polymers or rubbers was proved to be a more practical technology, due to the remarkable toughening effect and simple craft supporting. Although plenty of attempts have been performed to toughen PLA via melt-blending methods, attentions of researchers were used to be paid on the blends characterized by totally biodegradability. Indeed, the impact toughness have been increased somewhat, but not enough as the engineering plastics, since the improvements in impact toughness were not so exciting in aforementioned reports (As reports rarely stated the improvement on impact toughness was higher than 10 times[15]). Moreover, considering the relative higher price, it seemed not a cost effective method to toughen PLA with biodegradable polymers, especially for the purpose of PLA products used as commodity plastics in near future. Now, more and more traditional thermoplastic elastomers were taken as the impact modifier of PLA.[2,6] Although it might not be a long-term solution, it really provided an economic and viable means to meet the need of consumers. These materials were not only readily available and have excellent performances in general resins, but showed the tremendous toughening effects to PLA. For example, Su *et al.*[17] found that, PLA blended simply with 15% ethylene-α-octene copolymer (EOC) increased the impact toughness from 4.0 to 19.4 kJ/m^2. Moreover, with the aid of grafting

© 2016 Wiley Periodicals, Inc.

of glycidyl methacrylate (GMA) to EOC, a remarkable improvement by more than 12 times in impact toughness could be obtained.[17] Anderson *et al.*[18] stated that the addition of 20% linear low density PE (LLDPE) could heighten impact toughness more than 23 times. From the reports of Ma *et al.*,[19] PLA blended with poly(ethylene-*co*-vinyl acetate) (EVA) could obtain the impact toughness of 83 kJ/m^2, which was about 27 times higher than pristine PLA.

Ground tyre rubber (GTR) was well known as the production of waste tires. It was characterized by very low price and fine particle size, as has been utilized considerably as cheap impact resistance modifier in the plastic. Our previous study has focused on PLA/GTR blends, devoting to fabricating the PLA product with excellent impact toughness and high cost performance.[21] From the results, the PLA blend with 15% GTR showed the highest impact toughness and kind of declination in tensile strength and elastic modulus.[21] Moreover, we investigated the effects of styrene-butadiene-styrene block copolymer (SBS) on the morphological structures and mechanical properties. Although the impact toughness was increased steadily with SBS content, the tensile properties had a drastic decrease as the mass fraction of SBS beyond 15%.[22] By comparing our experimental results and the reports available, we found that different rubbery modifiers usually led to the various morphologies, and subsequently disparate physical and mechanical properties. It should be an interesting work, however, to make a detailed comparison on the toughening effects of different rubbery modifiers to PLA. Up to now, there was no literature was focused on this issue.

As well known, PLA was the polymer whose structure was characterized by repeated aliphatic ester structures. It was relatively easy to breakdown and hydrolyze, and usually exhibited poor thermal and photo-stability.[23,24] These characteristic properties, including thermal stability and thermal decomposition kinetics, of PLA were crucial and should be taken into the consideration during the determination of processing PLA products avoiding serious thermal decomposition. Recently, researchers have paid much attention on the thermal decomposition behavior of PLA and PLA blended with inorganic reinforcements. However, the reports available publicly of PLA toughened by elastomers were mainly emphasized on their structure−property relationships.[5,17–20] Few of them were focused on the thermal properties, especially the kinetics analysis of thermal decomposition.[21]

This study, therefore, was aimed at investigating the effects of various rubbery modifiers on the structures and properties of PLA. The GTR and SBS were chosen undoubtedly. Moreover, considering that EOC was a very popular thermoplastic elastomer applied in toughening PP, as well as PLA,[17] the EOC and GMA grafted EOC (mEOC) were also chosen as the impact modifiers in our experiments. PLA toughened with various rubbery modifiers were fabricated via melt-blending technology. Their morphologies, mechanical properties and thermal stabilities were investigated in detail. More important, the kinetics of thermal decomposition for all the samples were emphasized, and then kinetics parameters, such as activation energy and reaction order, were quantitative calculated based on the data of thermo gravimetric analysis (TGA).

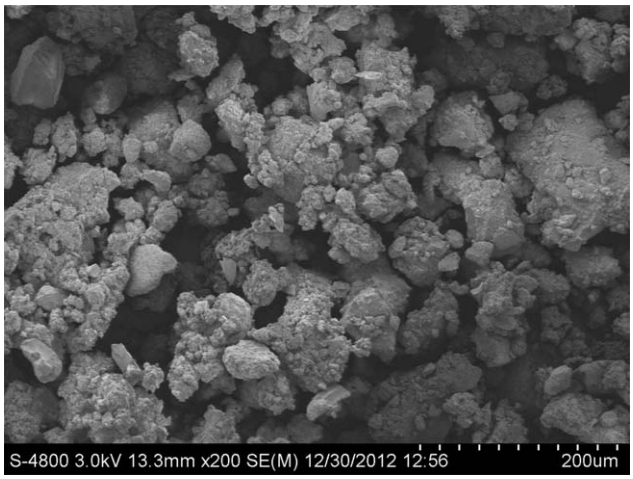

Figure 1. SEM micrograph of 120 mesh GTR.

EXPERIMENTAL

Raw Materials

PLA (REVODE101) was kindly supplied by Zhejiang Hisun Biomaterials (China). Its melt flow rate (MFR) was about 5.5∼10 g/10min, and the specific gravity was 1.25 g/cm^3. GTR purchased from Hangzhou Baoli Recycling (China). It was the blends of car and truck waste tires containing a small amount of fibers. The specific surface area of GTR was less than 0.1 m^2/g. SBS (4452) was the product of Sinopec Beijing Yanshan Company (China). It was oil-extended particle, of which the MFR was 2.5∼3.5 g/10 min. EOC (Engage 8180) was brought from DuPont Dow Chemical Company (USA). It was granular substance and the MFR equaled 0.5 g/10 min. mEOC (GP-7000), of which the MFR was 0.5∼2.5 g/10 min, was supplied by Suzhou Yasai Plastic & Chemical (China). The silane coupling agent used in this study was γ-aminopropyltriethoxysilane, which was usually named as KH-550. It was the product of Nanjing Shuguang Chemical Group, A.R. grade. Absolute alcohol and silicone oil were both commercial available with A.R. grade.

Fabrication of Samples

Before use, the dried GTR was passed through a sieve of 120 meshes, and then immersed into the alcohol solution contained 1.5 vol % KH550. The mixture was then stirred vigorously for about 4 h at 313.15 K, and then filtered, washed with deionized water and subsequently dried to constant weight in a vacuum oven. Finally, the silane agent treated GTR particles were obtained (as shown in Figure 1). Other thermoplastic elastomers were applied as received. Based on our previous studies,[21,22] all the rubbery modifiers were fixed at 15%, and the components for samples were listed in Table I. Materials were dried, respectively, in a vacuum oven at 333.15 K for at least 24 h for the removal of moisture before compounding. The blends were fabricated using a double-roll open mill. The PLA and rubbery modifiers were blended and compounded at 403.15 K for about 30 min. Then the melted mixtures were laid into the mold and compressed into sheets. The temperature and pressure were 418.15 K and 15 MPa, respectively, and the dimension of sheet was 200 mm for length and width and

Table I. Formulations of PLA Blends (wt %)

Samples	PLA	SBS	WRP	EOC	mEOC
Pristine PLA	100	–	–	–	–
PLA/GTR	85	15	–	–	–
PLA/SBS	85	–	15	–	–
PLA/EOC	85	–	–	15	–
PLA/mEOC	85	–	–	–	15

4 mm for thickness. As a control sample, neat PLA was undergone the same procedure. These as-molded sheets were then cut into sufficient specimens with required shapes and dimensions for the subsequent mechanical tests.

Characterization

All the mechanical measurements were conducted at room temperature. The tensile and impact tests were employed to determine the mechanical properties of pristine PLA and its blends. Uniaxial tensile tests were performed in a computer aided universal testing machine (WDW-50, China) following the Chinese Standards GB/T 1040.1-2006. Specimen with the shape of standard dumbbell (1A type) was taken for tensile testing. During the measurement, the gauge length of specimen was 50 mm and the testing speed was 2 mm/min. The tensile strength, elastic modulus and elongation at break of investigated samples were obtained as the outputs from the computer. According to Chinese Standards GB/T 1043.1-2008, Charpy impact tests of un-notched bar specimens were done in an impact tester (TCL-25J, China). The sample size was 80 × 10 × 4 mm^3, with the span length of 62 mm during the tests. From the test result, impact energy could be recorded directly. Then, impact toughness was calculated via dividing the impact energy by the cross-sectional area of the sample. All of the mechanical investigations were carried out with at least five duplications in each series. Only the standard deviation of testing results lower than 10% were recorded, and their average values were utilized to evaluate the samples' performance.

The fractured surfaces of sample from impact tests were selected for the observation of interfacial morphologies of PLA blended with various rubbery materials. Micrographs were taken in a field emission scanning electron microscopy (SEM, S-4800, Hitachi, Japan), of which the accelerating voltage was 3.0 kV. The non-conductive samples were coated with a thin layer of gold (about 10 nm) by sputtering technique before SEM examination. The resulted images were then analyzed by Image Pro Plus software, and the particles of second phase were counted. The average diameters (d_{MN}), standard deviation (SD), as well as coefficient of variation (CV) for each sample were calculated for characterizing the particle size and their dispersion state quantitatively. The CV value represented the uniformity of particles. The lower CV usually indicated a more homogenous distribution of particles of second phase.

Thermal properties of differential scanning calorimetry (DSC) and thermogravimetric analysis (TGA) were carried out by using the simultaneous DSC-TGA (SDT-2960, TA Instruments, USA) equipment. Tiny samples with about 10 mg were picked up directly from the core part of bar specimens. Tests were performed at a heating rate of 10 K/min from 323.15 to 823.15 K. The testing atmosphere was nitrogen (N_2), of which the flow rate was 60 mL/min. For each sample, the non-isothermal DSC and TGA curves were recorded by computer and then analyzed carefully. Finally, the characteristic thermal parameters could be obtained.

RESULTS AND DISCUSSION

Morphologies

Figure 2 presented the representative morphologies of PLA blended with various rubbery modifiers, as were selected from the samples fractured at room temperature during the impact tests. From these pictures, the interfacial morphologies and distribution of rubbery modifiers could be observed clearly. From Figure 2(a), the GTR behaved as the second phases and dispersed randomly in PLA matrix. The interfaces between GTR and PLA seemed blurry without obvious interfacial de-bonding. The GTR particles were mainly inlaid into the polymer, with

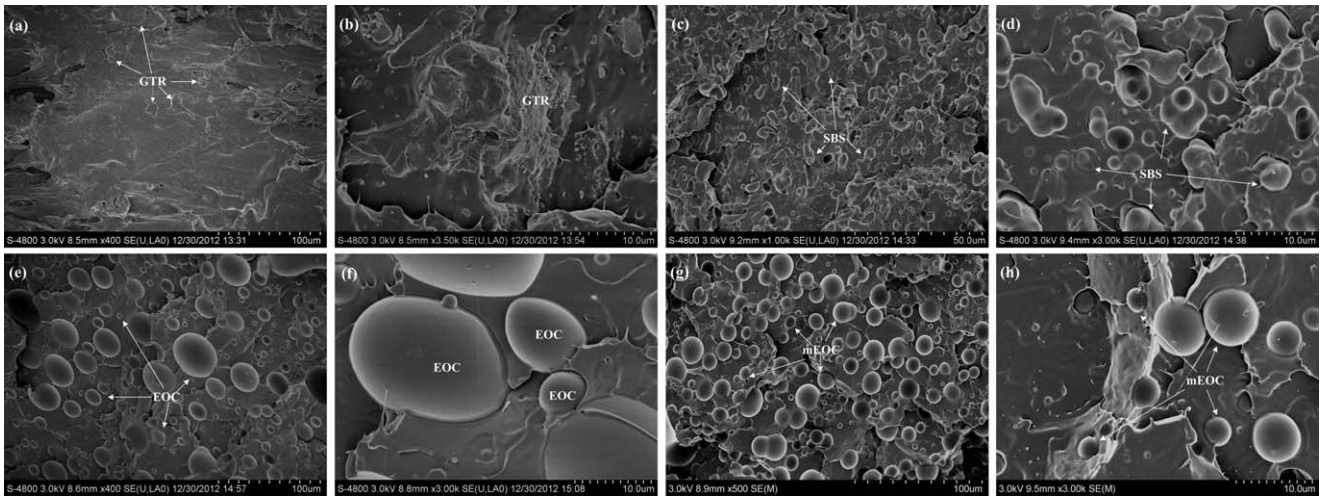

Figure 2. Morphological structures of PLA blends with varied rubbery modifiers: (a) PLA/GTR, (b) PLA/GTR with high magnification, (c) PLA/SBS, (d) PLA/SBS with high magnification, (e) PLA/EOC, (f) PLA/EOC with high magnification, (g) PLA/mEOC, and (h) PLA/mEOC with high magnification.

many small pieces dispersed around the larger blocks, as was demonstrated in the high magnification picture of Figure 2(b). Also, the well dispersed GTR particles were characterized by irregular shapes and sizes. Generally, the GTR possessed the cross-linking structures and hardly to be melted during the sample preparation.[25] The shear stress derived from the melt just had the possibility of dispersing the GTR, but could not break them. In fact, these small pieces should be closely related to the original morphologies of GTR. As could be seen in Figure 1, the GTR particles were characterized by large blocks adhered loosely with plenty of pieces. During the melt-blending, the shear stress of melt could separate these small pieces from the large blocks and scatter them in the polymer. Nevertheless, it might be very beneficial for improving the mechanical properties of materials, especially the impact toughness.

However, for the other three PLA/elastomer blends, the morphological structures showed a few differences on not only particle shapes, but particle size and the size distribution. Obviously seen in Figure 2(e–h), all the samples exhibited the typical droplet-matrix structures. PLA was acted as the continuous phase due to the relative higher MFR, while the thermoplastic elastomers with lower MFR were the hard phases, dispersing well in the matrix. The elastomeric particles were mainly spherical and showed relative clear boundaries with PLA, presenting the phase-segregating structures due to their incompatibility in nature. Figure 3 depicted the size distribution of SBS, EOC, and mEOC phases in the blends. The values of d_{MN}, SD, and CV for different elastomeric particles were also enclosed. Among the three elastomers, SBS showed the smallest average size, mEOC was the second, while EOC exhibited the biggest particle size. Their average diameters were 3.21 μm, 9.45 μm, and 13.94 μm, respectively. The sizes of SBS particles were located lower than 10 μm; however, the distribution range was 6∼50 μm for EOC and 1∼25 μm for mEOC domains. The narrowest distribution range, together with the lowest CV value shown in Figure 3(a), indicated the best uniformity of particle size distribution was obtained in PLA/SBS blend. In contrast, the PLA/EOC blend exhibited the worst state of dispersion on the elastomeric particle size accordingly.

Generally, in a heterogeneous blend system, the domains of second phase and their dispersion state should be affected largely by the melt viscosity of constituent components, under the same mass ratio and processing conditions. As well known, the melt viscosity of polymer was mainly related to many factors, including the molecular weight and distribution, structures, temperature, shear rate, shear stress, and the like. For determining the influences of these factors on the melt behavior, the complex rheological experiments were usually designed and proposed. However, in industry, the relative simplified measurement of MFR was used to be employed for representing the fluidity, i.e. the melt viscosity of polymers.[26] The higher MFR usually meant the lower melt viscosity. In the process of polymer blending, polymer melt (hard phase) with low viscosity tended to be more deformable and easily to be dispersed, and then the finer domains should be achieved. On the other hand, the interfacial compatibility also played an important role in the morphologies of blends. During the melt blending, as soon as the domains of

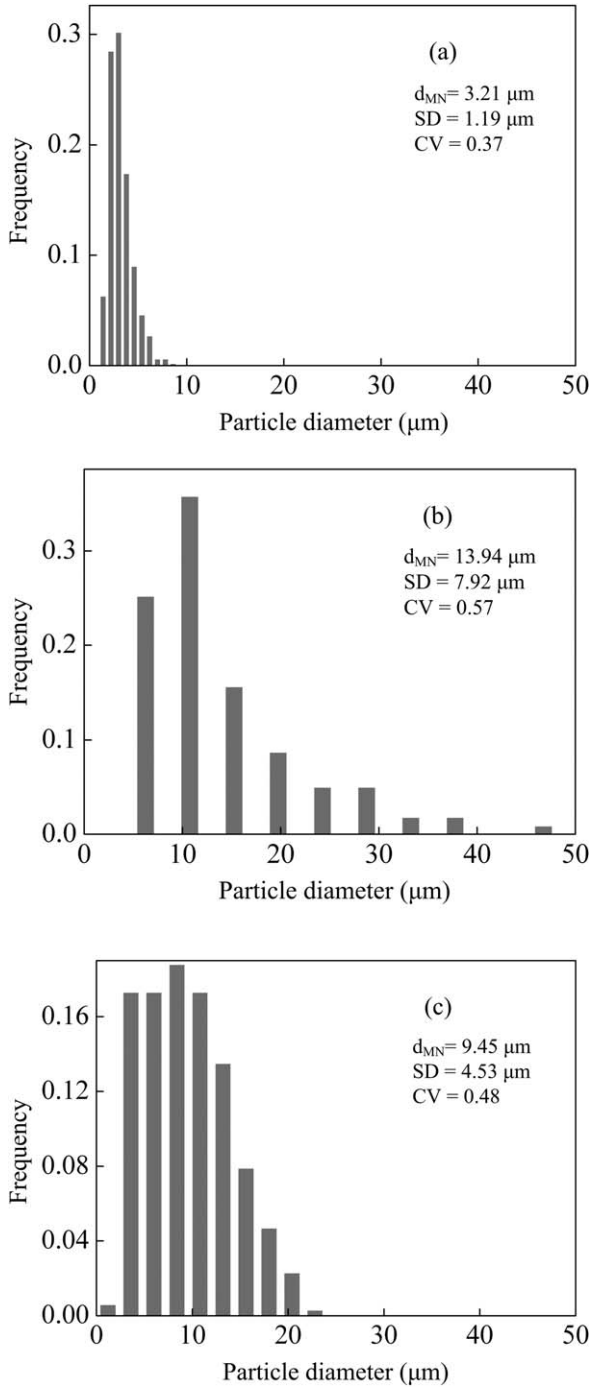

Figure 3. Size distribution of elastomeric particles for (a) PLA/SBS, (b) PLA/EOC, and (c) PLA/mEOC.

hard phase formed, there would be no hesitate to be wrapped and separated from each other by the continuous phase. And, the excellent compatibility between the continuous and dispersing phases usually showed the great possibility of preventing the fine domains from coalescing into large particles. Considering that the solubility parameter for PLA was 20.5 $MPa^{0.5}$,[27] for SBS was 19.0 $MPa^{0.5}$,[28] and for EOC was 17.5 $MPa^{0.5}$,[29] the SBS was certainly more compatible with PLA according to the like dissolves like theory. Then, the SBS domains, as soon as they formed,

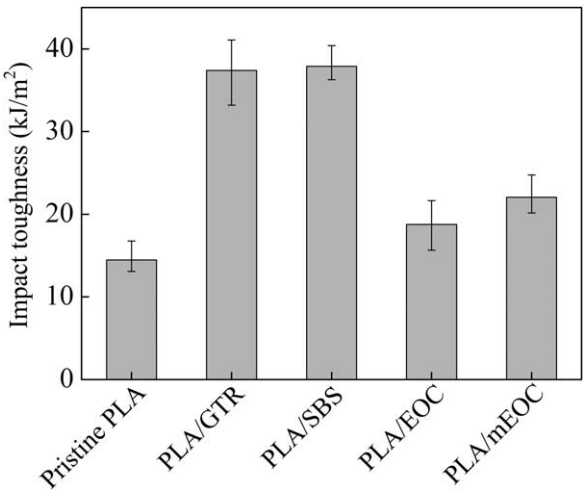

Figure 4. Impact toughness of pristine PLA and the blends.

could be effectively wrapped and separated from each other by PLA matrix. As a result, the highest MFR for SBS presented the finest particle size amongst the three elastomers. However, the EOC was a representative nonpolar polymer and certainly incompatible to PLA due to the obvious polar difference. Nevertheless, mEOC should be the more compatible to PLA than that of EOC due to the introduction of GMA groups. Although it was still not as great as that of SBS, it indeed could polarize the nonpolymer to some extent. Thus, the lowest MFR for EOC showed the largest domains, while mEOC was characterized by less average size of elastomeric particle than that of EOC.

Mechanical Properties

Figure 4 depicted the effects of different rubbery modifiers on the impact toughness of PLA blends. Clearly to see, all the modified samples exhibited higher impact toughness than that of neat PLA, showing the apparent toughening effects to PLA. In the investigated blends except for PLA/GTR, the PLA/SBS blend presented the highest value of 37.89 kJ/m^2, which showed an improvement by 161.9% in comparison to that of control sample (14.47 kJ/m^2). By contrast, the PLA/EOC and PLA/mEOC blends just obtained the improvements of 29.6% and 52.4%, respectively. This should be mainly ascribed to the introduction of soft elastomers. As well known, the elastomeric particles well dispersed in the matrix could act as stress concentration points, which were able to induce a lot of crazing and shear bands. Then, the excellent toughening effects should be demonstrated due to the interaction of crazing and shear bands.[30] Generally, the elastomeric particle with finer size and more amounts resulted in much more crazing and shear bands, and then more obvious toughening effect should be made. According to SEM observation, SBS presented the finest particle size, mEOC was second and EOC showed the biggest particles. It meant that much more elastomeric particles could be obtained in PLA/SBS blend when compared with PLA/EOC and PLA/mEOC cases, under the conditions of same mass fraction and similar relative densities (the densities for SBS was 0.92 g/cm^3, mEOC and EOC was 0.87 g/cm^3). So, the SBS should show more significant toughening effect for granted than that of EOC and mEOC. However, the enhanced interface compatibility between mEOC and PLA should have an important role in toughening the materials, and the PLA/mEOC blends showed higher impact toughness than that of PLA/EOC case. It has been demonstrated by Su *et al.*[18] and they emphasized that it was ascribed to the chemical reactions between the end carboxyl groups of the PLA and epoxy groups of the mEOC. But for PLA/GTR blend, it was more different due to its different intrinsic characteristic. As mentioned above, though the melt process wasn't able to shatter the GTR particles, it could scatter many small pieces in the matrix (the size was even lower than that of SBS). Therefore, the toughening effect was exhibited due to the theory of crazing and shear band.[30] However, another important factor would never be negative. The GTR usually contained many low molecular additives and the SBS was oil-extended, either additives or oil could migrate from GTR or SBS to the matrix during the melt-compounding process. Those low molecular matters might have additional toughening effects to PLA matrix. This might be the reason that the PLA/SBS and PLA/GTR blends obtaining the similar and relative higher impact toughness than that of PLA/EOC and PLA/mEOC cases.

The tensile properties including tensile strength, elastic modulus and elongation at break of pure PLA and the blends were shown in Figure 5. As could be seen, both of GTR and thermoplastic elastomers decreased the tensile strength and elastic modulus of PLA blends [Figure 5(a,b)]. It was reasonable according to rules of mixture. The modifiers employed in present experiment were rubbery nature and characterized by much lower strength and stiffness than that of PLA resin. Their introduction certainly showed the discourage influences on the tensile strength and elastic modulus of blends. Moreover, the decreased elastic modulus could also be viewed as the result of the lowering on the degree of crystallinity of the blends in relation to pure PLA.[31] Generally, the higher degree of crystallinity usually stood a higher elastic modulus of blends. However, the tensile strength was mainly related to the immiscibility of the components and the formation of bi-phase structures (seen in Figure 2), as has been reported by Van der Wal *et al.*[32] It was well known that the fracture process on the inter-phase was accelerated by the immiscibility of the components.[31] Therefore, it was the relative high degree of crystallinity and well bonded interface that made PLA/GTR blend have superior strength and stiffness than other blends. However, the inherent cross-linked structure should make GTR be possessed of higher strength and stiffness than other elastomers,[25] as might contribute to slowing down the negative effect of GTR on the mechanical properties.

As an indication of material ductility under the quasi-static loading, the elongation at break was also shown in Figure 5(c). Apparently, the pristine PLA was more brittle than other blends and displayed the least elongation at break (only 0.83%), as was in agreement with the impact toughness (shown in Figure 4). However, the effects of rubbery modifiers on the elongation at break were not exactly the same as that of impact toughness. Certainly, all the rubbery modifiers improved the flexibility, of which the PLA/SBS case was extremely amazing. Among the samples, the elongation at break for PLA/SBS blend was highest (8.02%), indicating the improvement by 866.3% higher than that of control sample. Despite of that, other rubbery modifiers

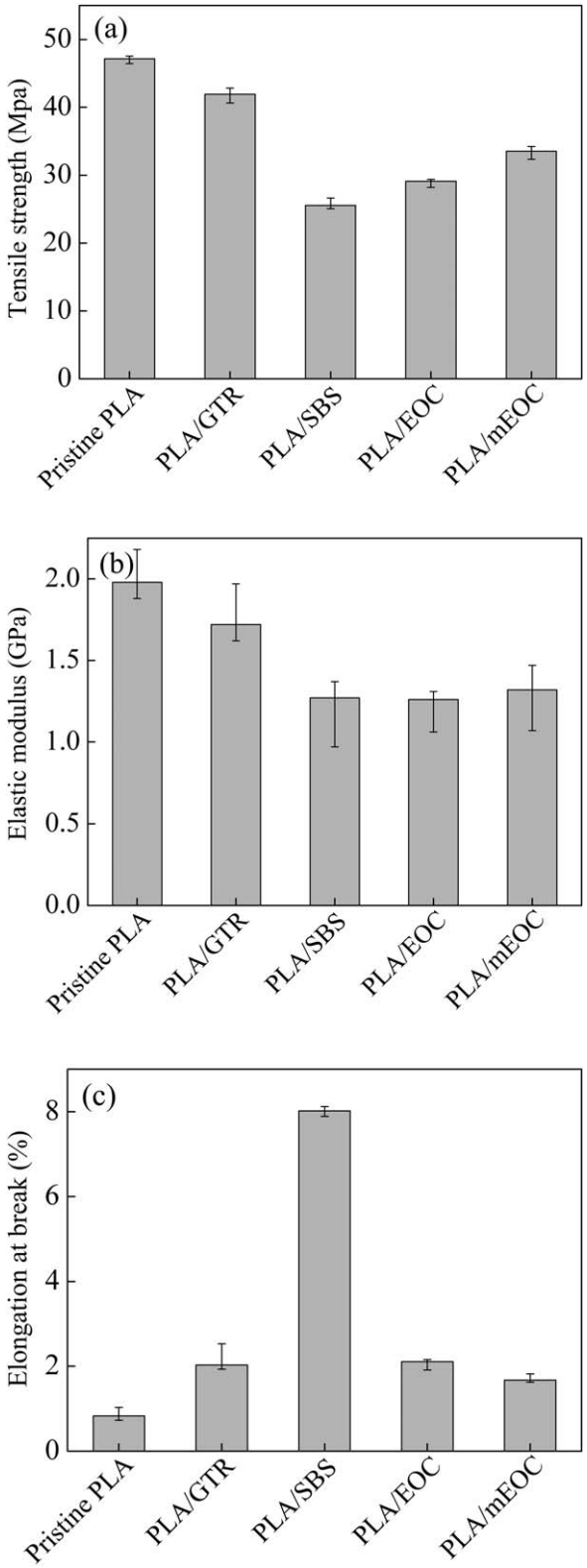

Figure 5. Tensile properties of pristine PLA and the blends: (a) tensile strength, (b) elastic modulus, and (c) elongation at break.

presented the similar improvements (about 100∼155%) on the elongation at break. Obviously, the influence of SBS on the elongation at break was much superior to that of other modifiers. It was understandable because the SBS was utilized as the oil-extended particles. During the melt compounding, the oil could be transmitted into the matrix and acted as the plasticizers, that offering the extra contributions on the ductility of materials. Nevertheless, the present experimental results were not as higher as that reported in Ref. 18, and therefore, some useful strategies should be proposed and performed in our further experiments.

Thermal Properties

Thermal properties were the most important macro properties of thermoplastics, as usually gave useful information about article service temperature range and processing (foaming, extrusion and injection) temperature range. Figure 6 illustrated the DSC heating curves of neat polymer and PLA blends with various rubbery modifiers. All the samples showed the broad melting behavior, and the temperature range of melting for blends were somewhat narrowed when compared to that of pristine PLA. The incorporation of rubbery modifiers seemed to have little influences on the peak temperatures of melting (T_{mp}), which were located at around 420.5 ± 2.0 K. However, the enthalpies of fusion for blends were decreased significantly, as was evidenced by the shrunk peaks. The degrees of crystallinity for PLA phase in investigated samples were calculated by the ratio between the enthalpy of fusion of the blend and the enthalpy of fusion of the perfect crystalline PLA (93.1 J/g[33]), which were also presented in Figure 6. It was noticed that the crystallinity for pure PLA was highest (69.9%), exhibiting the characteristic of representative semi-crystalline polymer. However, the degrees of crystallinity of PLA phases for blends decreased significantly, and 34.4% for PLA/GTR, 20.2% for PLA/SBS, 19.8% for PLA/EOC, and 22.8% for PLA/mEOC cases. It was believed that the rubbery matters could inhibit the motions of molecular chains, and then decreased the crystallization capacity of PLA phase. As was expected, because any changes in the degrees of crystallinity were the refection in variation of crystalline structures, which were then affected the mechanical properties of samples. Generally, the pristine PLA with much higher degree of crystallinity was possessed of

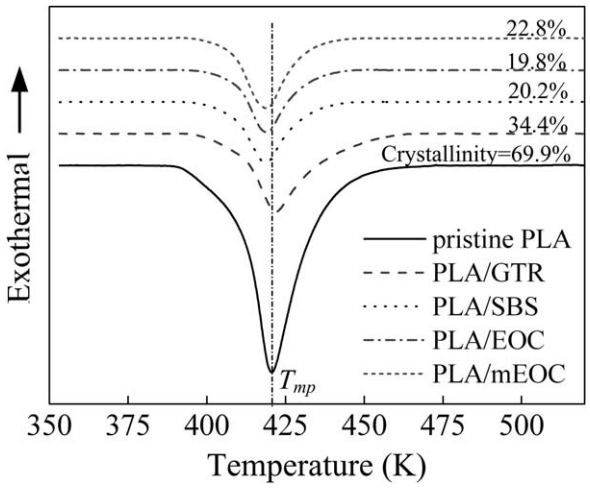

Figure 6. Melting behavior and the corresponding crystallinity of PLA phase for pristine PLA and the blends.

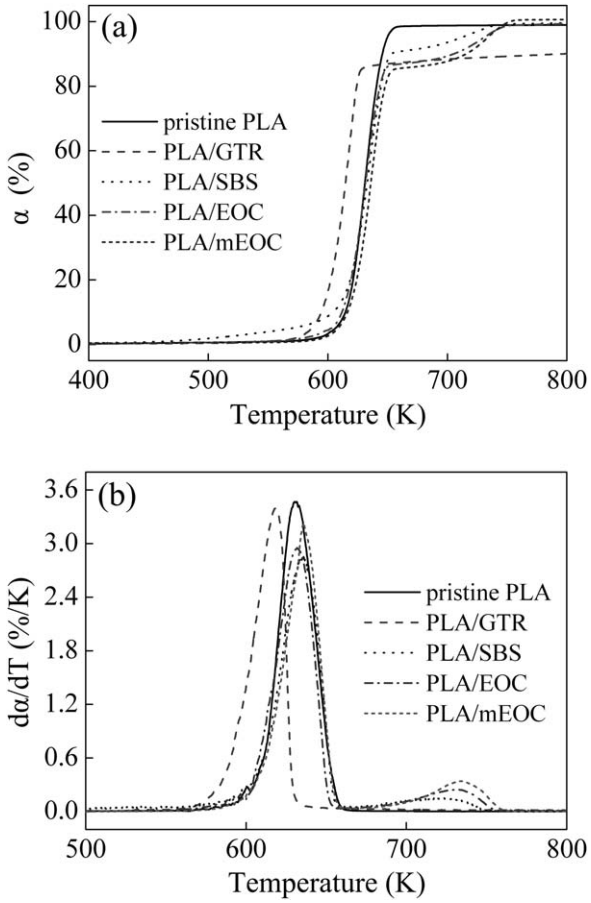

Figure 7. Thermograms of pristine PLA and the blends for (a) TGA and (b) DTG curves.

relative higher strength and stiffness, as was shown in Figure 5, whereas the blends preferred to be more flexible due to the dominant amorphous phases (seen in Figure 4). In addition, from the investigation of Chen *et al.*[34] and Li and Shimizu,[35] there should be cold crystalline peaks at around 385 K appearing in the DSC thermograms of PLA and the blends. They attributed this to the fact that polymer was cooled with a too fast cooling rate, which resulted in the crystalline far from perfect. However, there was no signal of cold crystallization behavior observed in present samples, as was very different from the reported results. This might be indicated that the employed preparing conditions of samples offered the sufficient cooling rate for the crystalline process of PLA phase. After all, the degree of crystallinity was as much as 69.9%, which was even higher than the sum of degrees of crystallinity derived from cold crystallization (29.8%) and melting (32.5%).[34]

Figure 7 depicted the variation of mass conversion (α) and first conversion derivative as a function of absolute temperature (T) for neat PLA and various blends, which were usually named as TGA and DTG thermograms, respectively. Table II collected some useful characteristic parameters for PLA phase which could be determined from TGA and DTG curves. Of which, T_i was the initial decomposition temperature ascertained by ISO method in TGA curve [Figure 7(a)], and T_p was the temperature at maximum rate of mass conversion, which was actually the temperature of peak in DTG curve [Figure 7(b)]. And, α_i and α_p represented the corresponding mass conversion, respectively. As be seen clearly, the investigated materials were thermally stable and showed sufficient resistance to weight loss up to processing temperatures (418.15 K), as gave the idea about the processing conditions and applications of such blends directly. The single step decomposition process was observed in both pristine PLA and PLA/GTR blends. However, the incorporation of GTR decreased the decomposition temperatures and increased the corresponding mass conversion. The T_i and T_p were reduced from 614.95 K and 630.80 K for neat PLA to 595.03 K and 618.59 K for PLA/GTR case, while the α_i and α_p were increased from 10.19% and 49.16% for neat PLA to 10.61% and 62.78% for the blend, respectively. It was indicated that GTR accelerated thermal degradation of PLA, as should be due to its relative lower thermal stability (shown in Figure 8). The thermal degradation behavior for GTR started from around 526.7 K, which was much lower than that of neat PLA. This could be ascribed to the fact that the low molecular matters (such as plasticizer, antioxidant, and other auxiliary agents) remained in GTR were volatilized before the polymer pyrolysis.

However, all the rest three blends exhibited the two step degradation with the first maximum decomposition peak around 635 K and second maximum decomposition peak higher than 710 K. Clearly, these two degradation process reflected each degradation behavior of the PLA and elastomer ingredients, suggesting the typical phase-segregation structures, as has been identified by SEM observations. Due to the oil with low boiling point that contained in SBS, the occurrence of mass conversion began early at lower than 500 K and showed obvious mass loss before the thermal cleavage of molecular chains (as shown in Figure 8). But, the peak temperature of polymer pyrolysis was much higher than that of neat PLA. As a result, the PLA/SBS blend presented a relative lower T_i but a higher T_p when compared with that of control sample, whereas the values of α_i and α_p were increased undoubtedly. The PLA/EOC and PLA/mEOC blends, however, showed the very similar thermal degradation behaviors because of their same backbone structures. Moreover, the curves for the two blends were very close to that of pristine PLA in the initial stage, as was confirmed by the very similar values of T_i in Table II. Nevertheless, the T_p for two blends showed the higher values than pure PLA due to the relative higher pyrolysis temperatures of EOC and mEOC. Interestingly, both of PLA/EOC and PLA/mEOC blends showed the decreased values of α_i, which was rather different from the PLA/GTR and

Table II. Characteristic Thermal Parameters of Samples[a]

Samples	T_i (K)	α_i (%)	T_p (K)	α_p (%)
PLA	614.95	10.19	630.80	49.16
PLA/GTR	595.03	10.61	618.59	62.78
PLA/SBS	609.74	12.33	635.79	58.08
PLA/EOC	611.62	9.67	632.86	53.98
PLA/mEOC	616.33	9.83	635.87	49.65

[a] These data were just for PLA phase.

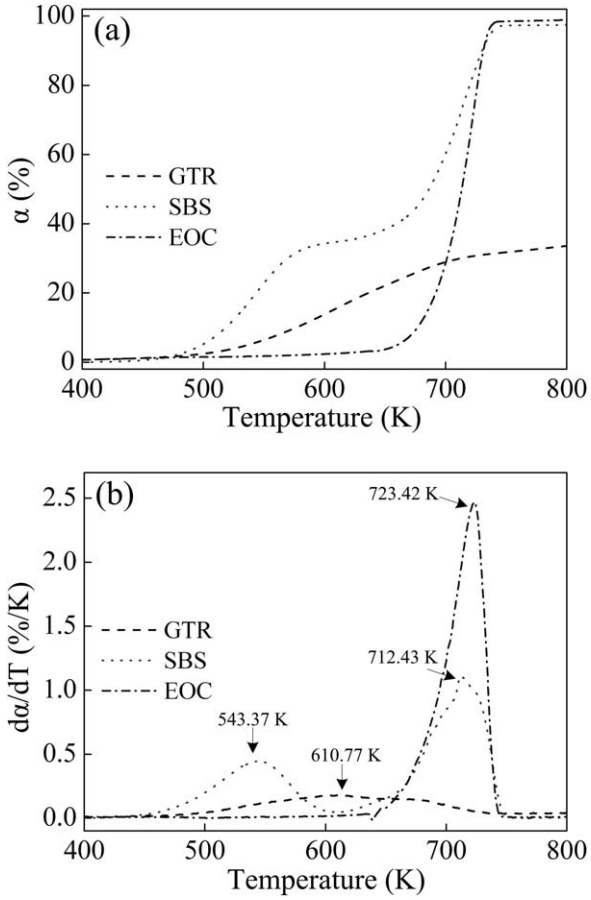

Figure 8. Thergrams of neat GTR, SBS, and EOC for (a) TGA and (b) DTG (The mEOC curves were overlapped with that of EOC and not depicted in present figures).

PLA/SBS cases. It was indicated that the introduction of either EOC or mEOC impeded the mass conversion of PLA phase in the initial stage. Despite of it, their values for α_p were a little higher than pure PLA, but much lower than that of PLA/GTR and PLA/SBS blends. It revealed the fact that, although the similar facilitating effects derived from EOC and mEOC on the thermal degradation of PLA phase were shown likewise, it was not so great in comparison with that of GTR and SBS.

Analysis of Decomposition Kinetics

In order to further understand the thermal degradation behavior of PLA and the blends, the data obtained from TGA and DTG curves could be used to determine the kinetic parameters of thermal degradation for various samples. Of which, the activation energy and reaction order should be of great essential. A lot of methods have been developed to analyze the kinetic parameters by using different approaches, such as integration, differentiation and approximation. Several researchers reported their calculated activation energy of PLA or the blends based on a series of TGA and DTG curves obtained at various heating rates, and the representative methods were Friedman,[36] Kissinger,[37] and Flynn-Wall-Ozawa[38,39] equations. However, because the degradation process of polymer was rate dependence (actually thermal hysteresis), an increase in heating rate usually led to a decomposition behavior of polymer shifting to higher temperature in TGA and DTG curves. In other words, the change in heating rate would bring on a different temperature range where decomposition of polymer took place. Considering that, Carrasco *et al.*[40] and Wang *et al.*[41] proposed the peak property method to determine the kinetic parameters by using the thermal degradation data with a unique heating rate, for the purpose of avoiding potential mechanism changes in both overall reaction order and activation energy. And this method was also employed in present study to analyze the activation energy and reaction order of the pristine PLA and the blends toughened by various rubbery modifiers.

As well known, the kinetics of thermal degradation of polymer was a function of temperature (T) and heating rate (β), which was typically expressed as follows:

$$\frac{d\alpha}{dT} = \frac{A}{\beta} \cdot \exp\left(-\frac{E}{RT}\right) \cdot f(\alpha) \tag{1}$$

where $d\alpha/dT$ was the mass conversion rate of polymer (%/K), and actually the values of vertical ordinate in Figure 7(b), A was the pre-exponential factor, E represented the activation energy (kJ/mol), R was the gas constant, and equaled 8.314 J/(mol·K), and $f(\alpha)$ was the kinetic model function and usually expressed as $(1-\alpha)^n$, where n was the reaction order.[42,43] Then, eq. (2) could be achieved by taking the derivative of eq. (1).

$$\frac{d^2\alpha}{dT^2} = \frac{d\alpha}{dT} \cdot \left(\frac{E}{RT^2} - \frac{n}{1-\alpha} \cdot \frac{d\alpha}{dT}\right) \tag{2}$$

Generally, when the maximum rate of thermal decomposition for sample was reached, the eq. (2) ought to be zero. And then, the expression, eq. (3), for activation energy could be obtained by, meanwhile, substituting the values T_p, α_p, and the maximum rate of mass conversion $(d\alpha/dT)_p$, which could be gotten from the TGA and DTG curves as shown in Figure 7.

$$E = \frac{nRT_p^2(d\alpha/dT)_p}{(1-\alpha_p)} \tag{3}$$

Apparently, to calculate activation energy, the reaction order of thermal degradation should be determined first. By involving eqs. (1)–(3) and the related peak values, reaction order could be

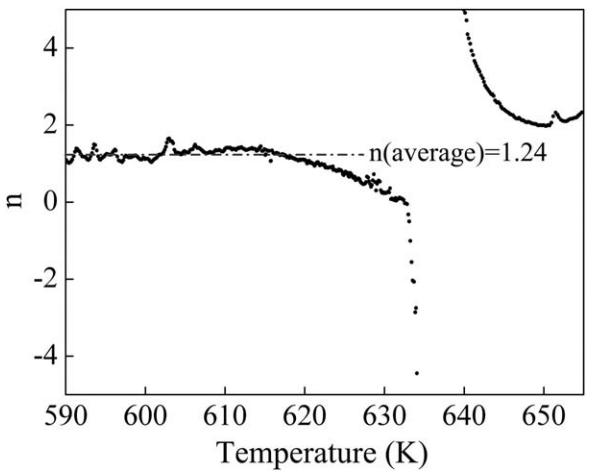

Figure 9. Reaction order as a function of temperature for pristine PLA.

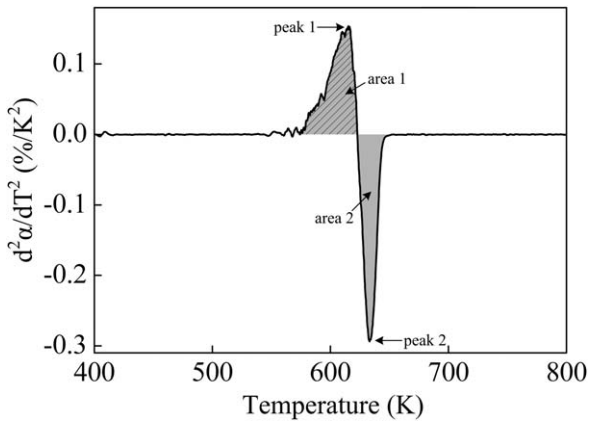

Figure 10. Second conversion derivative of TGA curves for pristine PLA.

expressed as a function of temperature, which was shown in eq. (4). Nevertheless, the value of reaction order was not a constant value, as was varied with the decomposition temperature. Figure 9 showed the representative relationship of n versus T for pristine PLA, which was plotted according to eq. (4). It was found that only during the first stage of thermal decomposition (from 590 to 615 K), the value of n presented the approximate constant at any mass conversion, with the average value of about 1.24. However, at the temperature near to T_p, the curve was discontinuous and tended to be infinite. It was impractical to use such changing n values to calculate the activation energy of samples.

$$n = \frac{\ln \frac{(d\alpha/dT)_p}{(d\alpha/dT)}}{\frac{T_p \cdot (T_p - T)}{T} \cdot \frac{(d\alpha/dT)_p}{1-\alpha_p} - \ln \frac{1-\alpha}{1-\alpha_p}} \quad (4)$$

According to Kissinger's conclusion,[37] the average reaction order of the overall thermal degradation could be estimated based on the measurement of peak asymmetry in DTG curves. He characterized asymmetry of DTG peak by using a shape factor (S), which was defined as the absolute value of the ratio of the slopes of the tangents to DTG curve at the inflexion points. Actually, it could be evaluated easily from the absolute ratio of the heights of peak 1 and peak 2 illustrated in Figure 10. Then, the reaction order was calculated according to $n = 1.26 \cdot S^{1/2}$. However, Carrasco and co-workers[40] argued that this equation was not accurate greatly because the influence of peak width was neglected. So, they developed an alternative novel procedure involving the peak area to calculate the reaction order, as the equation was shown as follows:

$$n = \frac{\int_{T_i}^{T_p} \frac{d^2\alpha}{dT^2} \cdot dT}{-\int_{T_p}^{T_f} \frac{d^2\alpha}{dT^2} \cdot dT} \quad (5)$$

Where T_f was the temperature mass conversion was finished. From eq. (5), the reaction order could be obtained via dividing the area1 by area 2 (absolute value) presented in Figure 10. The values of n and E for various samples calculated according to Kissinger and Carrasco methods, respectively, were summarized in Table III. According to Kissinger method, the reaction order was 0.912 for pristine PLA whereas it was 0.753 for PLA/GTR case and 1.00∼1.07 for the rest three modified PLA blends. Apparently, the introduction of GTR decreased the reaction order while other elastomers increased the reaction order. Similar trend of variation in the n values derived from Carrasco method was also exhibited. However, the values of n for pure PLA, PLA/GTR, and PLA/SBS cases were relative higher, while for PLA/EOC and PLA/mEOC cases were a little lower when compared to the corresponding n values based on Kissinger method. Moreover, the difference of n values between pure polymer and the blends based on Carrasco method was great smaller than that based on Kissinger method, as was evidenced by the much lower CV shown in Table III. As aforementioned description, the Kissinger method was mainly based on the shape factor (which was determined through heights of the two peaks in Figure 10), and the applied general coefficient (1.26) was totally independently of the reaction order. The resulted reaction order did not take into consideration the peak shape and width, as then should lead to much deviation in the calculated results. Nevertheless, the Carrasco method was involved the peak shape and width, and no corrector coefficient was needed. So, it might achieve the more accurate reaction order based on this method. In a word, the rubbery modifier showed little influence on the reaction order (Carrasco method), and the thermal degradation process of PLA phase in all samples followed the first order reaction.

Table III also presented the calculated values of the activation energy for PLA phase of various samples. The difference in E value calculated by the two methods could be explained by the substitution of different n value. It was found that all the blends showed lower E values than that of pristine PLA, as was independent on the method used. By using Kissinger n value, the E value of PLA/GTR blend was the lowest; however, it was only lower than that of pristine PLA, but higher than that of other blends according to Carrasco method. It was indicated that the improper n value resulted in the inaccurate E value. As well known, rubber ingredients that left in GTR could accelerate the breakdown of polymer chains and reduce the energy barrier.[21] However, GTR usually contained fillers of carbon black and inorganic particles, which could provide the tortuous path for diffusion of low molecular matter during the thermal

Table III. Reaction Order (n) and Activation Energy (E) for PLA Phase of Various Samples Calculated by Kissinger and Carrasco Methods

	Kissinger		Carrasco	
Samples	n	E (kJ/mol)	n	E (kJ/mol)
Pristine PLA	0.912	264.25	1.011	292.71
PLA/GTR	0.735	178.82	1.005	244.68
PLA/SBS	1.003	215.90	1.052	226.06
PLA/EOC	1.053	210.38	1.041	207.97
PLA/mEOC	1.066	229.57	1.038	223.47
	CV=0.128		CV=0.018	

decomposition.[44] As a result, the reduction in activation energy could be somewhat released and the highest *E* value among PLA blends was maintained undoubtedly. For the rest blends, it was found that the *E* value was closely related to the morphologies of the blends. The relative higher activation energy was belonged to the sample characterized by more enhanced interfacial adhesion, finer particle size, and narrowed size distribution. The PLA/SBS blend with minimum elastomeric particle size and most narrowed size distribution was possessed of relative higher *E* value of 226.06 kJ/mol, whereas PLA/EOC blend showed the relative lower *E* value of 207.97 kJ/mol. Usually, lower *E* value indicated the thermal decomposition process tended to happen more easily, as also supported the accelerating effects of rubbery modifiers on the thermal degradation of PLA phase.

CONCLUSIONS

In this paper, samples of PLA blended with various rubbery modifiers were fabricated, and then their morphological structures, mechanical properties as well as thermal performances were investigated. Several useful conclusions were drawn as follows:

(1) The typical droplet-matrix morphologies were observed for PLA blends, exhibiting obvious phase-segregating structures. Well bonded interfaces between GTR and PLA were shown, with lots of fine pieces around the large blocks. Moreover, PLA/SBS blend showed the smallest average particle size and most narrow range of size distribution, whereas PLA/EOC case had the largest average particle size and most broad size distribution.

(2) The flexibility of PLA was improved considerably by incorporation of four kinds of rubbery modifiers. Of which, SBS was possessed of most toughening effect to PLA, showing the highest impact toughness (37.89 kJ/m^2) and elongation at break (8.02%), as were improved by 161.9% and 866.3%, respectively, when compared to that of neat polymer. However, the tensile strength and elastic modulus for blends were decreased due to incorporation of rubbery modifiers.

(3) The rubbery modifiers presented little influences on the peak temperatures of melting for PLA phase. Nevertheless, the corresponding degrees of crystallinity were declined significantly. Kinetics analysis of thermal decomposition revealed that the reaction orders for blends were similar to that of pure PLA, and their values of activation energy declined, indicating the accelerating effects on the thermal decomposition for PLA phase in the blends.

ACKNOWLEDGMENTS

This work was supported by Anhui Province Post Doctoral Researchers in Scientific Research Projects (No: 2014B006), the National Natural Science fund of China (No: 51303004) and the Anhui Provincial Natural Science Research Projects in Colleges and Universities (No: KJ2013Z067).

REFERENCES

1. Nampoothiri, K. M.; Nair, N. R.; John, R. P. *Bioresour. Technol.* **2010**, *101*, 8493.
2. Liu, H. Z.; Zhang, J. W. *J. Polym. Sci. Part B: Polym. Phys* **2011**, *49*, 1051.
3. Arakawa, K.; Mada, T.; Park, S. D.; Todo, M. *Polym. Test.* **2006**, *25*, 628.
4. Yang, B. Polylactic Acid [M]; Beijing: Chemical Industry Press, **2007**, p 1. [in Chinese]
5. Hashima, K.; Nishttsuji, S.; Inoue, T. *Polymer* **2010**, *51*, 3934.
6. Anderson, K. S.; Schreck, K. M.; Hillmyer, M. A. *Polym. Rev.* **2008**, *48*, 85.
7. Perego, G.; Cella, G. D.; Bastioli, C. *J. Appl. Polym. Sci.* **1996**, *59*, 37.
8. Lemmouchi, Y.; Murariu, M.; Santos, A. M. D.; Amass, A. J.; Schacht, E.; Dubois, P. *Eur. Polym. J.* **2009**, *45*, 2839.
9. Ren, Z.; Dong, L.; Yang, Y. *J. Appl. Polym. Sci.* **2006**, *101*, 1583.
10. Theryo, G.; Jing, F.; Pitet, L. M.; Hillmyer, M. A. *Macromolecules* **2010**, *43*, 7394.
11. Okubo, K.; Fujii, T.; Thostenson, E. T. *Compos. A* **2009**, *40*, 469.
12. Bledzki, A. K.; Jaszkiewicz, A.; Scherzer, D. *Compos. A* **2009**, *40*, 404.
13. Murariu, M.; Ferreira, A. D. S.; Degée, P.; Alexandre, M.; Dubois, P. *Polymer* **2007**, *48*, 2613.
14. Hong, Z. K.; Zhang, P. B.; He, C. L.; Qiu, X. Y.; Liu, A. X.; Chen, L.; Chen, X. S.; Jing, X. B. *Biomaterials* **2005**, *26*, 6296.
15. Wang, R.; Wang, S.; Zhang, Y.; Wan, C.; Ma, P. *Polym. Eng. Sci.* **2009**, *49*, 26.
16. Zhang, N.; Wang, Q.; Ren, J.; Wang, L. *J. Mater. Sci.* **2009**, *44*, 250.
17. Su, Z. Z.; Li, Q. Y.; Liu, Y. J.; Hu, G. H.; Wu, C. F. *Eur. Polym. J.* **2009**, *45*, 2428.
18. Anderson, K. S.; Hillmyer, M. A. *Polymer* **2004**, *45*, 8809.
19. Ma, P.; Hristova-Bogaerds, D. G.; Goossens, J. G. P.; Spoelstra, A. B.; Zhang, Y.; Lemstra, P. J. *Eur. Polym. J.* **2012**, *48*, 146.
20. Zhang, H. L.; Liu, N. N.; Ran, X. H.; Han, C. Y.; Han, L. J.; Zhuang, Y. G.; Dong, L. S. *J. Appl. Polym. Sci.* **2012**, *125*, E550.
21. Yang, J. N.; Nie, S. B.; Ding, G. X.; Wang, Z. F.; Gao, J. S.; Zhu, J. B. *Int. Polym. Proc.* **2015**, *30*, 467.
22. Yang, J. N.; Xu, A. Q.; Cheng, G. J.; Yu, X. H. *J. Mater. Eng.* **2013**, *10*, 20. (in Chinese)
23. Södergård, A.; Näsman, J. H. *Polym. Degrad. Stab.* **1994**, *46*, 25.
24. Wachsen, O.; Platkowski, K.; Reichert, K. H. *Polym. Degrad. Stab.* **1997**, *57*, 87.
25. Adhikari, B.; De, D.; Maiti, S. *Prog. Polym. Sci.* **2000**, *25*, 909.
26. Da Silva, A. L. N.; Tavares, M. I. B.; Politano, D. P.; Coutinho, F. M. B.; Rocha, M. C. G. *J. Appl. Polym. Sci.* **1997**, *66*, 2005.

27. Tsuji, H.; Sumida, K. *J. Appl. Polym. Sci.* **2001**, *79*, 1582.
28. Jeong, J. K.; Lee, D. C. *Korea Polym. J.* **1996**, *4*, 9.
29. Han, S. J.; Lohse, D. J.; Condo, P. D.; Sperling, L. H. *J. Polym. Sci. Part B: Polym. Phys.* **1999**, *37*, 2835.
30. Jang, B. Z.; Uhlmann, D. R.; Vander Sande, J. B. *J. Appl. Polym. Sci.* **1985**, *30*, 2485.
31. Da Silva, A. L. N.; Rocha, M. C. G.; Coutinho, F. M. B.; Bretas, R. E. S.; Farah, M. *Polym. Test.* **2002**, *21*, 647.
32. Van der Wal, A.; Mulder, J. J.; Oderkerk, J.; Gaymans, R. J. *Polymer* **1998**, *39*, 6781.
33. Park, S. D.; Todo, M.; Arakawa, K.; Koganemaru, M. *Polymer* **2006**, *47*, 1357.
34. Chen, R. Y.; Zou, W.; Wu, C. R.; Jia, S. K.; Huang, Z.; Zhang, G. Z.; Yang, Z. T.; Qu, J. P. *Polym. Test.* **2014**, *34*, 1.
35. Li, Y. J.; Shimizu, H. *Macromol. Biosci.* **2007**, *7*, 921.
36. Friedman, H. L. *J. Polym. Sci. Part C* **1964**, *6*, 183.
37. Kissinger, H. E. *Anal. Chem.* **1957**, *29*, 1702.
38. Flynn, J. H.; Wall, L. A. *J. Res. Nat. Bur. Stand.* **1966**, *70A*, 487.
39. Ozawa, T. *J. Therm. Anal.* **1970**, *2*, 301.
40. Carrasco, F.; Pagès, P.; Gámez-Pérez, J.; Santana, O. O.; Maspoch, M. L. *Polym. Degrad. Stab.* **2010**, *95*, 2508.
41. Wang, G.; Li, A. M.; Jiang, R. X. *Acta Energiae Solaris Sinica* **2010**, *31*, 497. (in Chinese)
42. Khawam, A.; Flanagan, D. R. *J. Phys. Chem. B* **2006**, *110*, 17315.
43. Hu, R. Z.; Shi, Q. Z. Thermokinetic Analysis [M]; Science Press: Beijing, **2008**, p 10. (in Chinese)
44. Kim, H.; Abdala, A. A.; Macosko, C. W. *Macromolecules* **2010**, *43*, 6515.